An alternative assay to discover potential calmodulin inhibitors using a human fluorophore-labeled CaM protein

By: Martín González-Andrade, Mario Figueroa, Rogelio Rodríguez-Sotres, Rachel Mata, and Alejandro Sosa-Peinado

González-Andrade, M., Figueroa, M., Rodríguez-Sotres, R., Mata, R., Sosa-Peinado, A. (2009). An alternative assay to discover potential calmodulin inhibitors using a human fluorophore-labeled CaM protein. *Analytical Biochemistry, 387* (1), pp. 64-70. DOI: 10.1016/j.ab.2009.01.002

Made available courtesy of Elsevier: https://doi.org/10.1016/j.ab.2009.01.002

Abstract:

This article describes the development of a new fluorescent-engineered *human* calmodulin, *h*CaM M124C–mBBr, useful in the identification of potential calmodulin (CaM) inhibitors. An *h*CaM mutant containing a unique cysteine residue at position 124 on the protein was expressed, purified, and chemically modified with the fluorophore monobromobimane (mBBr). The fluorophore-labeled protein exhibited stability and functionality to the activation of calmodulin-sensitive *c*AMP phosphodiesterase (PDE1) similar to wild-type *h*CaM. The *h*CaM M124C–mBBr is highly sensitive to detecting inhibitor interaction given that it showed a quantum efficiency of 0.494, approximately 20 times more than the value for wild-type *h*CaM, and a large spectral change (~80% quenching) when the protein is in the presence of saturating inhibitor concentrations. Two natural products previously shown to act as CaM inhibitors, malbrancheamide (**1**) and tajixanthone hydrate (**2**), and the well-known CaM inhibitor chlorpromazine (**CPZ**) were found to quench the *h*CaM M124C–mBBr fluorescence, and the IC_{50} values were comparable to those obtained for the wild-type protein. These results support the use of *h*CaM M124C–mBBr as a fluorescence biosensor and a powerful analytical tool in the high-throughput screening demanded by the pharmaceutical and biotechnology industries.

Keywords: Calmodulin | Fluorophore-labeled CaM protein | Fluorescence assay | CaM inhibitors

Article:

Calmodulin (CaM)[1] is a small Ca^{2+}-modulated protein of 148 amino acids (16,706 Da) considered as the primary transducer of Ca^{2+}-mediated signals in eukaryotes. It has four motifs called EF hands (each bind a single Ca^{2+} ion) that are composed of two α-helices linked by a 12-

residue loop. CaM amino acid sequence is highly conserved in animal and plants, although the latter organisms express several CaM isoforms.

CaM acts on many cellular targets, including soluble enzymes, ion channels, and primary pumps, resulting in a variety of essential downstream cellular effects [1], [2], [3], [4], [5], [6]. Accordingly, this protein influences a number of important physiological processes representing an important drug target [7]. Indeed, many CaM inhibitors are well-known antipsychotic smooth muscle relaxants, antitumoral and α-adrenergic blocking agents, among others. The interaction of CaM with its physiological targets depends on the exposure of two hydrophobic pockets (Fig. 1) following the conformational change elicited by Ca^{2+} binding to the protein.

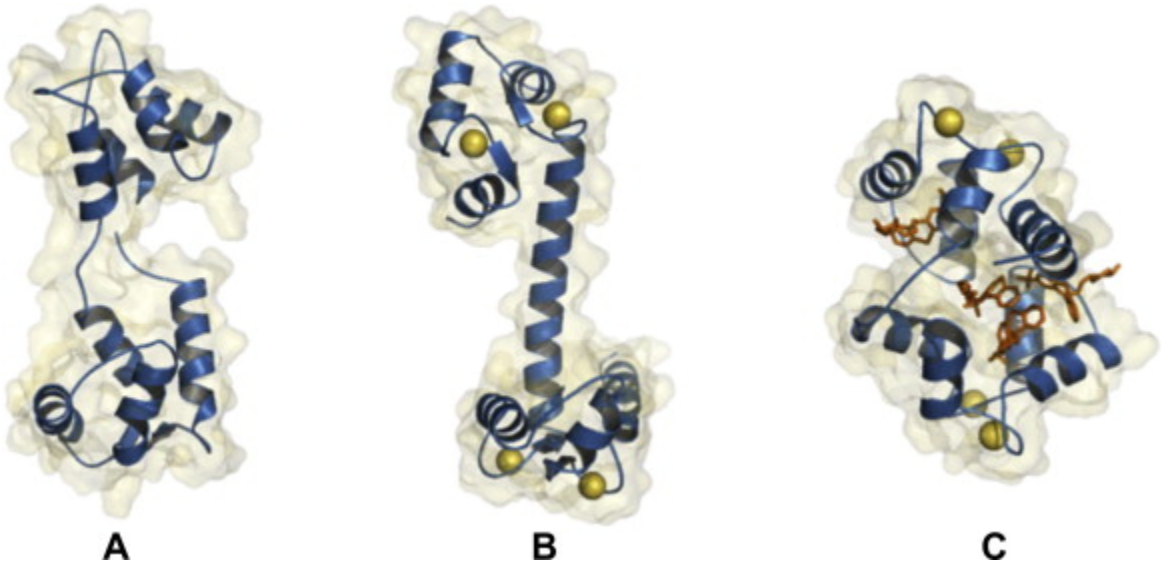

Fig. 1. Three-dimensional structures of CaM in its different conformations: (A) calcium free (Protein Data Bank [PDB] code: 1CFD); (B) with calcium (PDB code: 1CLL); (C) with TFP (PDB code: 1LIN). The structures were drawn using the PyMOL program [38].

Many compounds, including drugs, pesticides, and research tools, interact with CaM at the same hydrophobic sites also provoking conformational changes in the protein. Many of these substances behave as CaM antagonists, the best-known structural examples of these interactions are the antipsychotic analogs of trifluoroperazine (TFP) (Fig. 1) [8]. Such interactions can be detected using several analytical methods, including affinity chromatography, ultraviolet (UV), circular dichroism (CD) spectroscopy [9], gel electrophoresis [10], [11], nuclear magnetic resonance (NMR) [12], [13], X-ray diffraction [8], [14], [15], [16], functional enzymatic assays [17], [18], [19], and fluorescence-based technologies such as fluorescence resonance energy [20], [21], [22], [23]. The fluorescence-based methods are highly specific, low cost, selective, and they have rapid reaction time, although sometimes the preparation of the sensing element can be laborious. Among the fluorescence-based methods, the use of site-selective fluorescently labeled CaM has become popular recently. In addition, these methods have been demonstrated to be a powerful biosensing system for screening certain classes of drugs such as tricyclic antidepressants [24]. One of the most widely used procedures involves the covalent attachment to CaM of a thiol-reactive fluorophore strategically located using site-directed

cysteine mutagenesis. With such a molecular probe, it is possible to correlate the conformational changes with ligand binding by the changes in the emission properties of the labeled proteins.

In previous investigations, it has been determined that the attachment of different fluorophores at the cysteine residue located at position 109 produced better extrinsic fluoresce enhancement on ligand binding [25]. Here we describe the development of a fluorescence-based assay useful for detecting potential CaM inhibitors using a fluorescent *human* CaM (*h*CaM). The protein was engineered by rational design, replacing Met124 by cysteine using site-directed mutagenesis; the resulting protein, *h*CaM M124C, was purified by hydrophobic exchange chromatography and monobromobimane (mBBr) was attached covalently to Cys124 as fluorescent probe. The fluorophore mBBr was selected because of its high sensitivity. Such sensitivity has been successfully exploited in the elucidation of the secondary structure of T4 lysozyme [26]. The stability and functionality of *h*CaM M124C–mBBr (*h*CaM labeled with mBBr at position 124) were determined by CD measurement and functional enzymatic assay using calmodulin-sensitive *c*AMP phosphodiesterase (PDE1) as a monitor enzyme. Furthermore, the usefulness of *h*CaM M124C–mBBr was demonstrated by testing the ability of the known CaM inhibitors malbrancheamide (**1**), tajixanthone hydrate (**2**) [27], [28], and chlorpromazine (**CPZ**) (Fig. 2) to quench the fluorescence of the engineered protein and to inhibit CaM–PDE1 complex.

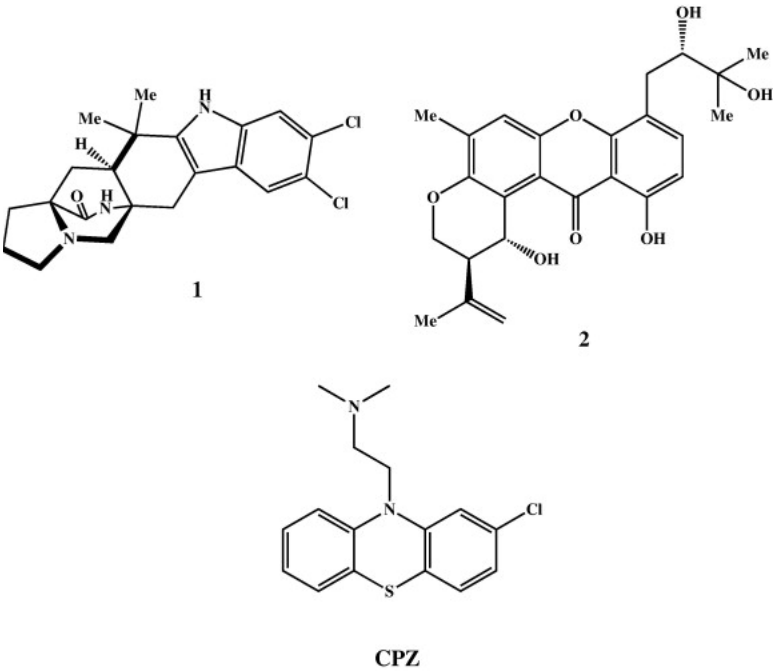

Fig. 2. Structures of compounds **1**, **2**, and **CPZ**. The structures were drawn with ChemBioDraw software (version 11.0, CambridgeSoft, http://www.cambridgesoft.com).

Materials and methods

Reagents

CALM1 (human phosphorylase kinase, delta) gene was purchased from Origene Technology (Rockville, MD, USA). pGEM-T Easy Vector System I was purchased from Promega (Madison,

WI, USA). pET12b vector was obtained from Novagen (Darmstadt, Germany). Pfu DNA polymerase was purchased from Stratagene (La Jolla, CA, USA). *Nde*I and *Bam*HI were obtained from New England Biolabs (Ipswich, MA, USA). Primers for polymerase chain reaction (PCR) mutagenesis and *Escherichia coli* BL21-AI One Shot were purchased from Invitrogen (Carlsbad, CA, USA). mBBr was purchased from Toronto Chemical Research (Toronto, Canada). All other reagents were of analytical reagent grade and were purchased from Sigma (St. Louis, MO, USA).

Subclonig of gene encoding for *h*CaM and site-directed mutagenesis

CALM1 gene encoding *h*CaM was amplified using PCR from the complementary DNA (cDNA) clone pCMV6-XL5 (Origene Technology) along with the primers (5′-CATATGGCTGATCAGCTGACCG-3′ and 5′-CCTAGGAGTAAAACGTCAGTAGT AGAC-3′) to insert restriction sites *Nde*I and *Bam*HI at the start and end of the gene. Amplified products were cloned into a vector (pGEM-T Easy Vector System I) and further subcloned into the protein expression vector pET12b Novagen (EMD Chemicals, Darmstadt, Germany). Single amino acid substitutions were generated by overlapping PCR mutagenesis using the Quick Change Kit (Stratagene). All clones and mutations were confirmed by nucleotide sequencing with an ABI PRISM 310 Genetic Analyzer (Applied Biosystems, Foster City, CA, USA). In all cases, the single methionine at position 124 in the wild-type sequences was replaced by cysteine to facilitate conjugation of the reporter group to this thiol. Plasmids were transformed into *E. coli* BL21-AI One Shot following the specifications of the kit's manufacturer.

Protein purification of *h*CaM and the mutant *h*CaM M124C

A single colony of *E. coli* strain BL21-AI/pET12b was grown in Luria–Bertani (LB) medium containing 100 mg/ml of ampicillin overnight with shaking at 37 °C and was inoculated into 500 ml of LB medium containing 100 mg/ml of ampicillin until the optical density (OD) of the culture at 550 nm reached between 0.8 and 1.0. Expression was induced by the addition of l-(+)-arabinose (0.2%, w/v) overnight with shaking at 37 °C. The cells were harvested by centrifugation (10 min, 4000*g*), resuspended in 50 mM Tris–HCl, 2 mM ethylenediaminetetraacetic acid (EDTA), 1 mM dithiothreitol (DTT), and 200 mg/ml of egg white lysozyme at pH 7.5 and were chilled on ice for 30 min. Resuspended cells were lysed by sonication, and cellular debris was removed by centrifugation for 15 min at 15,000*g.* The supernatant was collected, and $CaCl_2$ and NaCl were added to final concentrations of 5 and 500 mM, respectively. The protein was purified using a Phenyl Sepharose CL-4B chromatographic column. Briefly, the supernatant was applied to the column preequilibrated with 50 mM Tris–HCl, 0.5 mM DTT, 0.1 mM $CaCl_2$, and 500 mM NaCl at pH 7.5. The column was washed with loading buffer, followed by the same with 1 mM EDTA and 150 mM NaCl. Finally, the protein was loaded on a cationic exchange column (Source Q, Amersham Biosciences, Piscataway, NJ, USA) at pH 8.8 and was eluted by a linear gradient of 40 min (0–100%) with 500 mM NaCl. Protein was collected in fractions and assessed for purity by gel electrophoresis. All preparations were at least 98% pure by this criterion (Fig. 3).

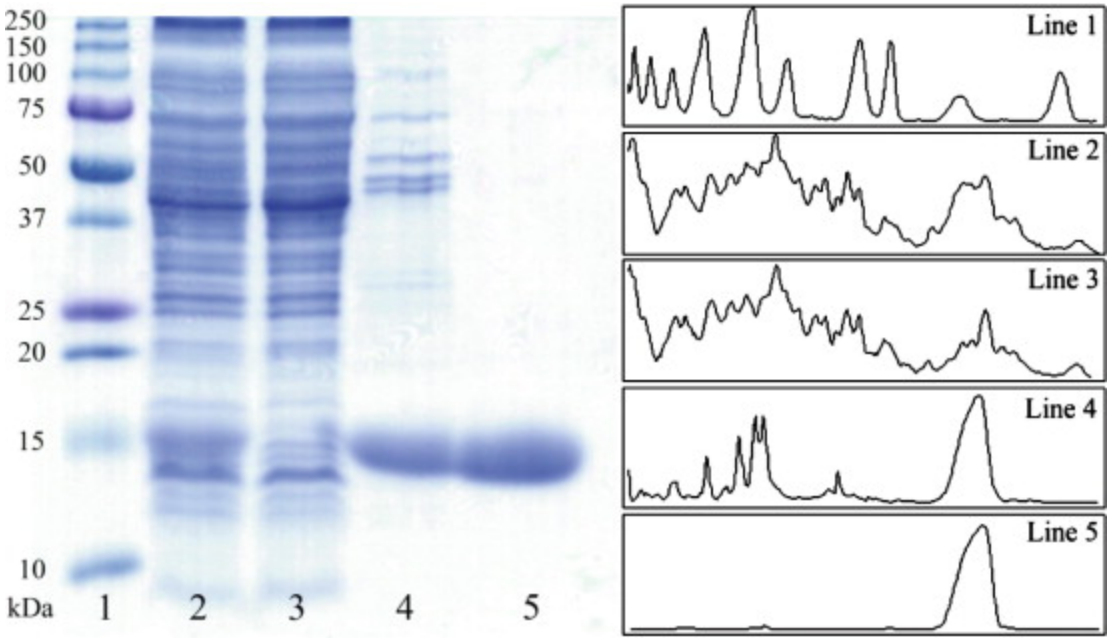

Fig. 3. Purification of *h*CaM M124C by sodium dodecyl sulfate–polyacrylamide gel electrophoresis (SDS–PAGE) and line profiles. Line 1: molecular weight standard proteins; line 2: supernatant of lysate; line 3: fraction nonbound at Phenyl Sepharose CL-4B column; line 4: fraction bound at Phenyl Sepharose CL-4B column; line 5: *h*CaM after cationic exchange column. The densitometric profiles were obtained using ImageJ software (http://rsb.info.nih.gov/ij).

Chemical modification of unique reactive cysteine of *h*CaM M124C protein with mBBr

All fluorophore conjugations steps were typically carried out at room temperature. To a protein at a concentration of 5 to 10 mg/ml, 5 mM was added and incubated for 3 h to reduce intramolecular disulfide bonds, and then it was washed on a gel filtration HR-100 column (Pharmacia Biotech, Piscataway, NJ, USA). A thiol-reactive fluorophore (20% in dimethyl sulfoxide [DMSO]) was added in small aliquots to reach a final concentration of 10 molar excess and DMSO of approximately 5%. Conjugation proceeded in the dark overnight at 4 °C. Separation of protein from unreacted fluorophore was achieved by size exclusion chromatography (Superdex 75). The efficiency of report group attachment was assessed by reactivity of the protein against 5-5′-dithiobis-(2-nitrobenzoic) acid (DTNB), measuring the release of 2-nitrobenzoate (TNB). Next, protein concentrations of both wild-type and labeled *h*CaM were determined with the bicinchoninic acid method [29].

Circular dichroism

CD wavelength scans and thermal melting data were recorded on a JASCO J-715 spectropolarimeter under an N_2 atmosphere with an attached thermal Peltier temperature control module. Thermal denaturation of *h*CaM wild-type and *h*CaM M124C–mBBr was monitored at 222 nm with a resolution step of 0.5 °C, a bandwidth of 1.0 nm, and a response time of 16 s. The concentration of protein used was 5 μM in 100 mM sodium phosphate buffer (pH 5.1). The sample was heated at a rate of 60 °C/h from 20 to 90 °C. Data were analyzed using the spectra

manager software (version 1.50.00) supplied with the instrument and using a nonlinear regression analysis to a two-state model with the Origin 7.0 program (OriginLab, Northampton, MA, USA):

$$\theta = \frac{(\theta_N + m_N[T]) + (\theta_N + m_U[T])e^{-(\Delta H_m/RT + \Delta H_m/RT_m)}}{1 + e^{-(\Delta H_m/RT + \Delta H_m/RT_m)}}, \quad (1)$$

where θ_N and θ_U represent the molar ellipticity in the native and unfolded states, respectively; m_N and m_U represent the temperature dependence of the molar ellipticity in the native and unfolded states, respectively; T represents temperature (K); R represents ideal gas constant (kcal mol^{-1} K^{-1}); ΔH represents change in enthalpy (kcal mol^{-1} K^{-1}); and T_m represents melting temperature (K).

Steady-state fluorescence

All measurements were conducted with an ISS–PC1 spectrofluorometer (ISS, Champaign, IL, USA) with sample stirring at 37 °C. The protein *h*CaM M124C–mBBr (5 μM) was incubated in buffer (100 mM phosphate [pH 5.1] and 10 mM $CaCl_2$). Fluorescence emission spectra were acquired with excitation and emission slit widths of 4 and 8 nm, respectively. The excitation wavelength was 381 nm, and emission wavelengths of 420 to 640 nm were measured. The fractional degree of saturated *h*CaM M124C–mBBr with ligand (y) was calculated by changes in fluorescence on ligand binding according to $y = (F - F_0) / (F_\infty - F_0)$, where F_∞ represents the fluorescence intensity at saturation of the ligand, y is plotted as a function of the inhibitor concentration, and the apparent dissociation constants (K_d) were obtained by fitting to Eq. (2):

$$y = \frac{(1 + K_d/P_0 + L_0/P_0) - \sqrt{(1 + K_d/P_0 + L_0/P_0)^2 - 4L_0/P_0}}{2}, \quad (2)$$

where y represents the fractional degree of fluorescence intensity at 470 nm, K_d is the apparent dissociation constant for the ligands, and P_0 and L_0 are the total concentrations of the protein and ligand, respectively. The data were analyzed using the Origin 7.0 program.

***h*CaM–PDE1 bioassay**

*h*CaM–PDE1 assay was performed in a 96-well plate as described previously [30] with some modifications. Briefly, wild-type *h*CaM or *h*CaM M124C–mBBr (0.08 μg) was incubated with 0.015 units of CaM-deficient/CaM-dependent *c*AMP phosphodiesterase from bovine brain for 30 min in 40 μl of assay solution containing 0.063 units of 5′-nucleotidase, 45 mM Tris–HCl, 5.6 mM magnesium acetate, 45 mM imidazole, 2.5 mM calcium chloride, and 10 μM bovine serum albumin (BSA) at pH 7.0. Test compounds were then added to the assay medium at 0.5, 1, 2, 3, 4, 7, 13, 20, 32, 50, and 65 μM in acetonitrile (ACN)/water (1:1), and the samples were incubated for 30 min. After that, 10 μl of 10.8 mM *c*AMP was added to start the assay. After 15 min, the assay was stopped by the addition of 190 μl of Malachite green solution. The phosphodiesterase reaction was coupled to the 5′-nucleotidase (*Crotalus atrox* venom from Sigma) reaction; the amount of inorganic phosphate released, measured spectrophotometrically at 700 nm, was correlated with the activity of the PDE1. All of the results are expressed as the mean of at least six experiments ± standard error of the mean (SEM). The IC_{50} values were

determined by nonlinear regression analysis performed with the Origin 7.0 program as reported previously [28].

Results and discussion

Design of a suitable site for *h*CaM mutagenesis

The specificity of the interaction of CaM with its molecular targets and its role in the regulation of several biochemical processes make this protein a powerful research tool to explore its physiological role and a target for drug discovery. Therefore, we have specifically labeled a cysteine residue at 124 with mBBr, a sensitive fluorescent probe, to yield a new *h*CaM variant (Fig. 4) following a rational approach with the goal of preserving the structural and functional properties of the native protein. The cysteine residue was introduced exchanging Met124 by site-directed mutagenesis. This position was selected for the following reasons. First, X-ray analyses of cocrystallized CaM-Ca^{2+}–TFP complex indicated the participation of 14 side chains in the binding site [25], including Met124; specifically, this position interacts with two molecules of TFP (Fig. 4). Furthermore, when TFP binds to CaM-Ca^{2+}, residue Met124 moves from being totally exposed to a buried position near the hydrophobic pocket (Fig. 4). Second, Met124 is located in a relative rigid α-helical region; therefore, disruption in the native fold of the protein for the formation of disulfide-linked aggregates is unlikely. This position also shows a large chemical shift change in the ^{1}H and ^{13}C NMR spectra when the protein is titrated with the inhibitor W-7 [31]. Therefore, the microenvironment surrounding position 124 is very susceptible to CaM inhibitors. Accordingly, attachment of a fluorophore at this position should report any conformational change on the inhibitor binding. Third, we carried out in silico studies of the modified protein using the HyperChem 7.5 program. When the structure was minimized to a 0.09 kcal/mol gradient with the AMBER94 force field, the linear distances from the thiol group of Cys124 (Cys124 SG) to N1 of each TFP molecule present in the Ca^{2+}-CaM–TFP complex were 3.75 and 4.96 Å, respectively. These distances were small enough to allow fluorescent quenching by the inhibitors but large enough to pose no severe steric hindrance on binding of a medium-sized ligand. Fourth, the solvent accessibility of *h*CaM M124C calculated by the Lee–Richards algorithm implemented in NACCESS 2.1.1 software [32] was 60.5 $Å^2$; thus, the inclusion of a small fluorophore such as mBBr should not affect its stability [26]. In summary, modification at position 124 was in agreement with previous work described in the literature [26], [33].

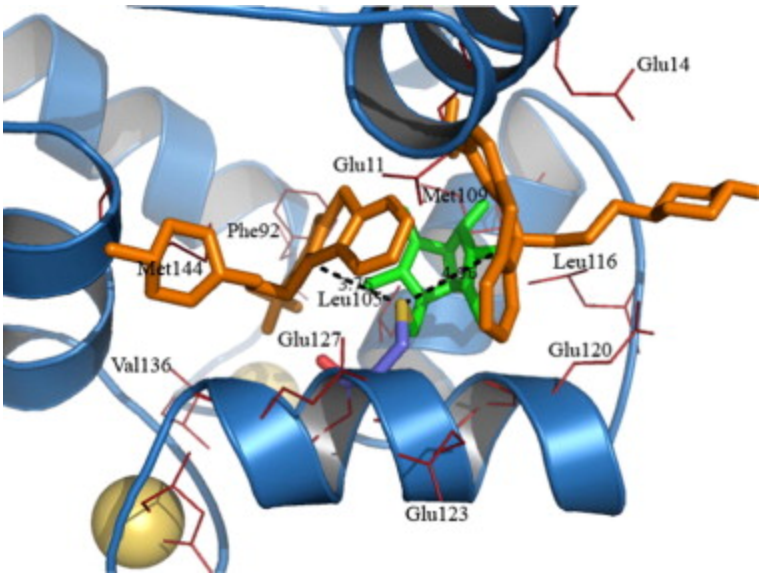

Fig. 4. In silico model of the mutation of cysteine residue and bimane attachment (*h*CaM M124C–mBBr) created using HyperChem software (version 7.5, HyperCube, http://www.hyper.com), by a geometric optimization using the AMBER force field, reaching a minimum gradient of 0.01 kcal $Å^{-1}$ mol^{-1}. Red lines show amino acid of the site binding in the CaM–TFP complex, green sticks show mBBr, orange sticks show TFP, and pale yellow balls show Ca^{2+}. Hydrogens are omitted for clarity.

The *h*CaM M124C was generated as described in Materials and methods and was chemically modified to give the corresponding *h*CaM M124C–mBBr.

Stability and functionality of *h*CaM M124C–mBBr

The folding, stability, and functionality of both the wild-type and mutant *h*CaM M124C–mBBr were studied by monitoring structural changes in the overall conformation using physical methods [34], [35] (far-UV CD) and an enzymatic assay. The percentages of secondary structure elements calculated from the far-UV CD spectra of both wild-type and *h*CaM M124C–mBBr do not show significant variations (84.27% α-helix and 1.24% β-structure) (Fig. 5A). The T_m values of wild-type *h*CaM and *h*CaM M124C–mBBr were 61 and 57 °C, respectively, suggesting thermal stability in both cases (Fig. 5B). The modified protein also displayed a significant activation of the PDE1. The IC_{50} values obtained for **CPZ** by PDE1 assays are consistent with those reported previously in the literature [9], [36], [37] (Table 1).

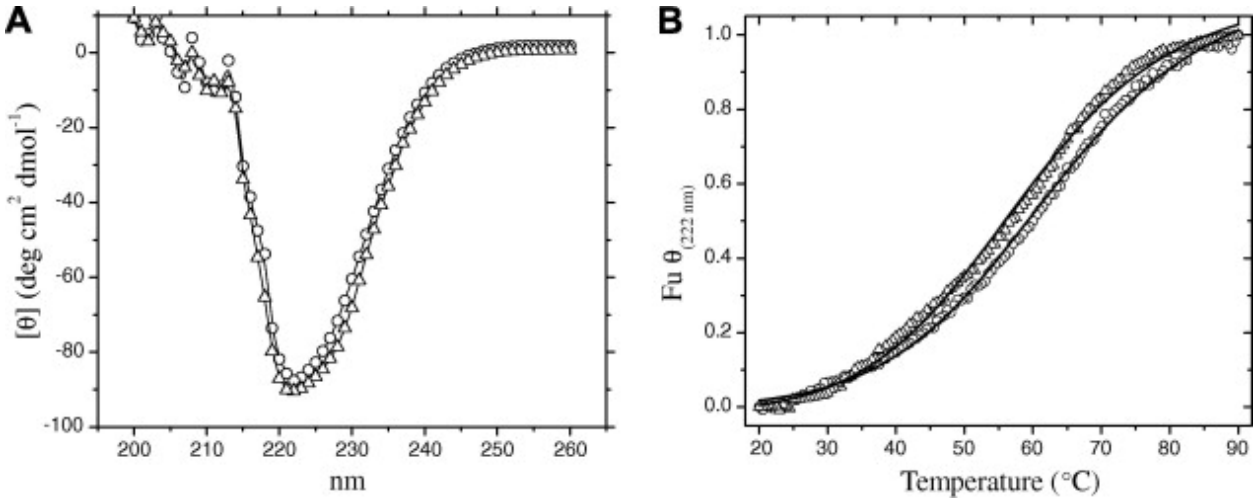

Fig. 5. Far-UV CD spectra (A) and molar ellipticity at 222 nm (B) for Apo-*h*CaM WT (○) and *h*CaM M124C–mBBr (Δ). The secondary structures in the presence of Ca^{2+} were determined from CD spectra using K2D2 program [39]. Thermal denaturation for both proteins were monitored by the changes in molar ellipticity as a function of the temperature, from 20 to 90 °C. The buffer was 100 mM sodium phosphate (pH 5.1). The solid lines are the best fits using Eq. (1) (see Materials and methods).

Table 1. Experimental IC_{50} values and apparent K_d values of compounds **1**, **2**, and **CPZ** determined by PDE1 and fluorescent assays.

Compound	***h*CaM WT**	***h*CaM M124C–mBBr**	
	IC_{50} (μM)[a]	**IC_{50} (μM)[a]**	**K_d (μM)[b]**
1	3.65 ± 0.74	3.04 ± 0.11	0.261 ± 0.023
2	5.62 ± 1.25	5.58 ± 0.20	0.033 ± 0.006
CPZ	21.98 ± 1.94	19.20 ± 0.36	1.714 ± 0.184

[a] Determined by PDE1 assay.
[b] Determined by fluorescent assay.

Titration of *h*CaM M124C–mBBr with compounds 1, 2, and CPZ

The modified protein showed a quantum efficiency of 0.494, approximately 20 times more than the value for wild-type *h*CaM (ϕ = 0.025). *h*CaM M124C–mBBr displayed the largest fluorescence response at 470 nm (λ_{ex} = 381 nm), thereby avoiding any interference due to UV absorption of most common ligands.

Fig. 6 and Table 1 summarize the concentration-dependent effect of compounds **1**, **2**, and **CPZ** on the fluorescence response of *h*CaM M124C–mBBr. The addition of compound **2** and **CPZ** quenched the fluorescence of the engineered protein in approximately 84%, whereas compound **1** showed a slightly smaller response (78%). In all cases, the effect correlated with the structural changes of the protein on binding of the inhibitor (Fig. 4, Fig. 6).

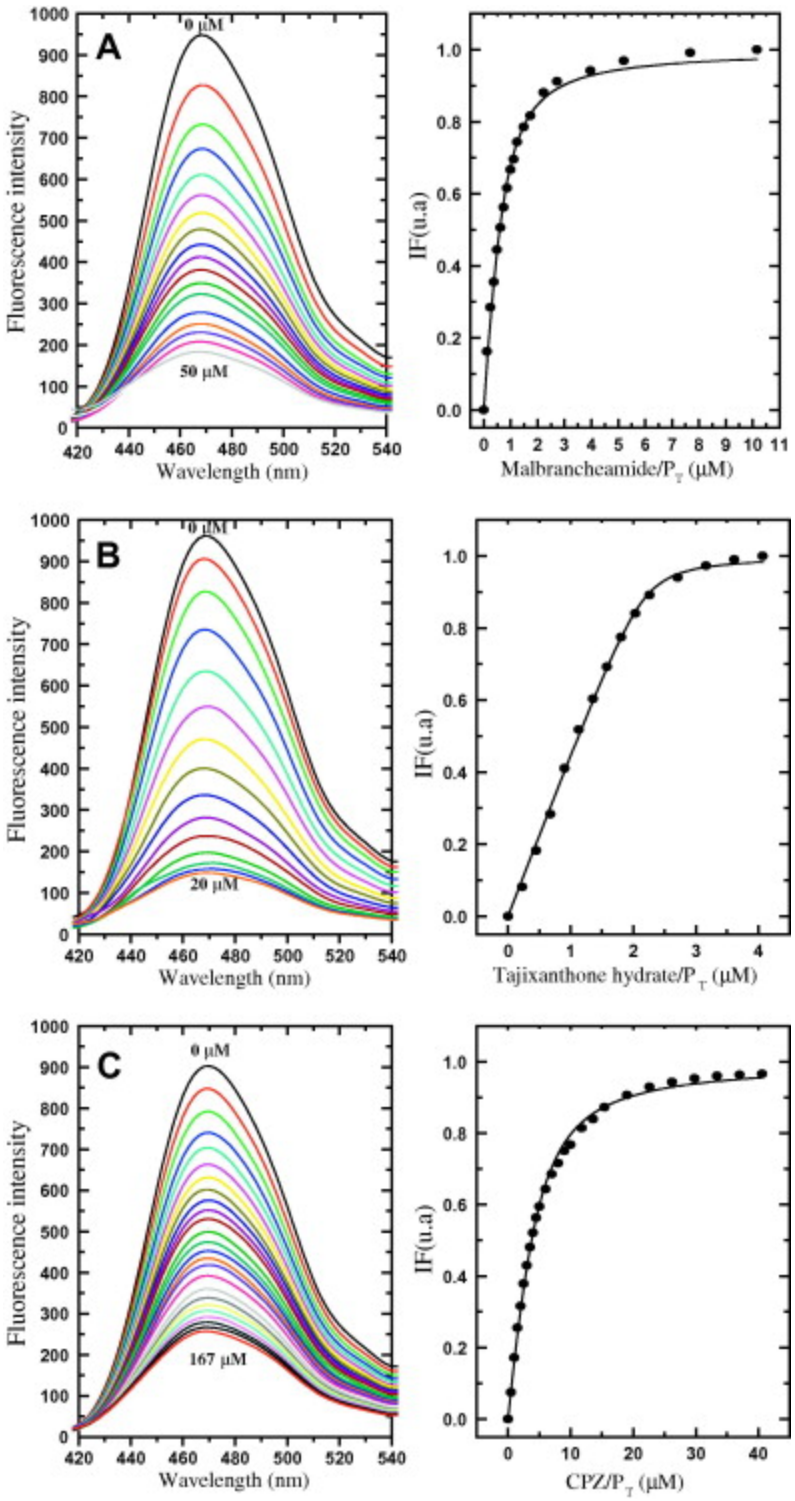

Fig. 6. Titration by fluorescence of engineered *h*CaM with compounds **1** (A), **2** (B), and **CPZ** (C) (left panels). Buffer was 5 mM KAc (pH 5.1) at 37 °C and 1 mM $CaCl_2$, and excitation was at 381 nm. The absolute changes of fluorescence emission at 470 nm (ΔΔIF) were plotted against the ratio inhibitor/protein and fitted to the binding equation model to obtain the fractional degree of saturated *h*CaM M124C–mBBr (right panels).

The signal changes maximal in fluorescence (470 nm) was plotted versus the inhibitor/protein total ratio, and the fitting curves provided an apparent K_d (see Materials and methods). The K_d of **CPZ** was similar to that reported previously for antagonists of the CaM [40]. The IC_{50} values calculated for **CPZ**, **1**, and **2** were consistent with those previously reported [9], [27], [36] and those found in the current study with native *h*CaM (Table 1), providing an important evidence of the specificity of *h*CaM M124C–mBBr.

Conclusions

A new fluorescent-engineered *h*CaM, *h*CaM M124C–mBBr, has been designed by a combination of site-directed mutagenesis and covalent attachment of a fluorophore probe. The protein is stable and functional for activation of PDE1 and shows promise for detecting new CaM inhibitors in a reliable, quick, and sensitive manner. The fluorophore-labeled protein detects classic CaM inhibitors such as **CPZ** and was used strategically for reevaluating two natural products. Its efficacy was demonstrated by means of a functional enzymatic assay and by fluorescence spectroscopy. Finally, *h*CaM M124C–mBBr can be used as an important tool for identifying new CaM inhibitors that will be useful as potential drugs or pesticides. Another possibility not tested in this work is to use *h*CaM M124C–mBBr to detect new potential protein–protein interactions given that this protein conserved functionality to interact with PDE1.

Acknowledgments

This work was supported by grants from Dirección General de Asuntos del Personal Académico (DGAPA, IN216207) and Consejo Nacional de Ciencia y Tecnologia (CONACyT, 53633 and 41328Q). The technical assistance of Isabel Rivero-Cruz is also recognized. M.G.A. acknowledges a fellowship for Ph.D. studies from CONACyT.

References

[1] E. Carafoli, C.B. Klee, Calcium as a Cellular Regulator, Oxford University Press, New York, 1999.

[2] M. Zhang, T. Yuan, Molecular mechanisms of calmodulin's functional versatility, Biochem. Cell Biol. 76 (1998) 313–323.

[3] H. Weinstein, E.L. Mehler, Ca2+-binding and structural dynamics in the functions of calmodulin, Annu. Rev. Physiol. 56 (1994) 213–236.

[4] R.E. Zielinski, Calmodulin and calmodulin-binding proteins in plants, Annu. Rev. Plant Physiol. Plant Mol. Biol. 49 (1998) 697–725.

[5] K.T. O'Neil, W.F. DeGrado, How calmodulin binds its targets: sequence independent recognition of amphiphilic a-helices, Trends Biochem. Sci. 15 (1990) 59–64.

[6] M.J. Berridge, M.D. Bootman, H.L. Roderick, Calcium signalling: dynamics, homeostasis, and remodelling, Nat. Rev. Mol. Cell Biol. 4 (2003) 517–529.

[7] R. Dagher, C. Pigault, D. Bonnet, D. Boeglin, C. Pourbaix, M.C. Kilhoffer, P. Villa, C.G. Wermuth, M. Hibert, J. Haiech, Use of a fluorescent polarization based high throughput assay to identify new calmodulin ligands, Biochim. Biophys. Acta 1763 (2006) 1250–1255.

[8] B.G. Vertessy, V. Harmat, Z. Bocskei, G. Naray-Szabo, F. Orosz, J. Ovadi, Simultaneous binding of drugs with different chemical structures to Ca2+– calmodulin: crystallographic and spectroscopic studies, Biochemistry 37 (1998) 15300–15310.

[9] S. Martinez-Luis, A. Perez-Vasquez, R. Mata, Natural products with calmodulin inhibitor properties, Phytochemistry 68 (2007) 1882–1903.

[10] M. Charpenteau, K. Jaworski, B.C. Ramirez, A. Tretyn, R. Ranjeva, B. Ranty, A receptor-like kinase from Arabidopsis thaliana is a calmodulin-binding protein, Biochem. J. 379 (2004) 841–848.

[11] B. Liao, M.C. Gawienowski, R.E. Zielinski, Differential stimulation of NAD kinase and binding of peptide substrates by wild-type and mutant plant calmodulin isoforms, Arch. Biochem. Biophys. 327 (1996) 53–60.

[12] J.J. Chou, S. Li, A. Bax, Study of conformational rearrangement and refinement of structural homology models by the use of heteronuclear dipolar couplings, J. Biomol. NMR 18 (2000) 217–227.

[13] D.J. Lalor, T. Schnyder, V. Saridakis, D.E. Pilloff, A. Dong, H. Tang, T.S. Leyh, E.F. Pai, Structural and functional analysis of a truncated form of Saccharomyces cerevisiae ATP sulfurylase: C-terminal domain essential for oligomer formation but not for activity, Protein Eng. 16 (2003) 1071–1079.

[14] R. Chattopadhyaya, W.E. Meador, A.R. Means, F.A. Quiocho, Calmodulin structure refined at 1.7 Å resolution, J. Mol. Biol. 228 (1992) 1177–1192.

[15] H. Kuboniwa, N. Tjandra, S. Grzesiek, H. Ren, C.B. Klee, A. Bax, Solution structure of calcium-free calmodulin, Nat. Struct. Biol. 2 (1995) 768–776.

[16] T. Okubo, S. Okada, Kinetic analyses of colloidal crystallization in alcoholic organic solvents and their aqueous mixtures as studied by reflection spectroscopy, J. Colloid Interface Sci. 204 (1998) 198–204.

[17] S.P. Chock, C.Y. Huang, An optimized continuous assay for cAMP phosphodiesterase and calmodulin, Anal. Biochem. 138 (1984) 34–43.

[18] A.C. Harmon, H.W. Jarrett, M.J. Cormier, An enzymatic assay for calmodulins based on plant NAD kinase activity, Anal. Biochem. 141 (1984) 168–178.

[19] R.K. Sharma, J.H. Wang, Preparation and assay of the Ca2+-dependent modulator protein, Adv. Cyclic Nucleotide Res. 10 (1979) 187–198.

[20] M.W. Allen, R.J. Urbauer, A. Zaidi, T.D. Williams, J.L. Urbauer, C.K. Johnson, Fluorescence labeling, purification, and immobilization of a double cysteine mutant calmodulin fusion protein for single-molecule experiments, Anal. Biochem. 325 (2004) 273–284.

[21] B. Sharma, S.K. Deo, L.G. Bachas, S. Daunert, Competitive binding assay using fluorescence resonance energy transfer for the identification of calmodulin antagonists, Bioconj. Chem. 16 (2005) 1257–1263.

[22] E. Dikici, S.K. Deo, S. Daunert, A whole-cell assay for the high throughput screening of calmodulin antagonists, Anal. Bioanal. Chem. 390 (2008) 2073–2079.

[23] J.P. Gangopadhyay, Z. Grabarek, N. Ikemoto, Fluorescence probe study of Ca2+- dependent interactions of calmodulin with calmodulin-binding peptides of the ryanodine receptor, Biochem. Biophys. Res. Commun. 323 (2004) 760–768.

[24] P.M. Douglass, L.L. Salins, E. Dikici, S. Daunert, Class-selective drug detection: fluorescently-labeled calmodulin as the biorecognition element for phenothiazines and tricyclic antidepressants, Bioconj. Chem. 13 (2002) 1186–1192.

[25] L.C. Vesna Schauer-Vukasinovic, S. Daunert, Rational design of a calcium sensing system based on induced conformational change of calmodulin, J. Am. Chem. Soc. 119 (1997) 11102–11103.

[26] S.E. Mansoor, H.S. McHaourab, D.L. Farrens, Determination of protein secondary structure and solvent accessibility using site-directed fluorescence labeling: studies of T4 lysozyme using the fluorescent probe monobromobimane, Biochemistry 38 (1999) 16383–16393.

[27] M. Figueroa, M.C. González, R. Rodríguez-Sotres, A. Sosa-Peinado, M. González-Andrade, C.M. Cerda-García-Rojas, R. Mata, Calmodulin inhibitors from the fungus Emericella sp., Bioorg. Med. Chem. (in press), doi:10.1016/j.bmc.2008.10.079.

[28] S. Martínez-Luis, L. Acevedo, M.C. González, R. Rodríguez-Sotres, A. Lira-Rocha, R. Mata, Malbrancheamide, a new calmodulin inhibitor from the fungus Malbranchea aurantiaca, Tetrahedron 62 (2006) 1817–1822.

[29] P.K. Smith, R.I. Krohn, G.T. Hermanson, A.K. Mallia, F.H. Gartner, M.D. Provenzano, E.K. Fujimoto, N.M. Goeke, B.J. Olson, D.C. Klenk, Measurement of protein using bicinchoninic acid, Anal. Biochem. 150 (1985) 76–85.

[30] B. Rivero-Cruz, I. Rivero-Cruz, R. Rodriguez-Sotres, R. Mata, Effect of natural and synthetic benzyl benzoates on calmodulin, Phytochemistry 68 (2007) 1147–1155.

[31] M. Osawa, M.B. Swindells, J. Tanikawa, T. Tanaka, T. Mase, T. Furuya, M. Ikura, Solution structure of calmodulin–W-7 complex: the basis of diversity in molecular recognition, J. Mol. Biol. 276 (1998) 165–176.

[32] B. Lee, F.M. Richards, The interpretation of protein structures: Estimation of static accessibility, J. Mol. Biol. 55 (1971) 379–400.

[33] R.M. de Lorimier, J.J. Smith, M.A. Dwyer, L.L. Looger, K.M. Sali, C.D. Paavola, S.S. Rizk, S. Sadigov, D.W. Conrad, L. Loew, H.W. Hellinga, Construction of a fluorescent biosensor family, Protein Sci. 11 (2002) 2655–2675.

[34] R.R. Biekofsky, S.R. Martin, J.E. McCormick, L. Masino, S. Fefeu, P.M. Bayley, J. Feeney, Thermal stability of calmodulin and mutants studied by 1H–15N HSQC NMR measurements of selectively labeled [15N] Ile proteins, Biochemistry 41 (2002) 6850–6859.

[35] L. Masino, S.R. Martin, P.M. Bayley, Ligand binding and thermodynamic stability of a multidomain protein, calmodulin, Protein Sci. 9 (2000) 1519–1529.

[36] S.Z. Khan, C.L. Longland, F. Michelangeli, The effects of phenothiazines and other calmodulin antagonists on the sarcoplasmic and endoplasmic reticulum Ca2+ pumps, Biochem. Pharmacol. 60 (2000) 1797–1806.

[37] M. Figueroa, M.C. González, R. Mata, Malbrancheamide B, a novel compound from the fungus Malbranchea aurantiaca, Nat. Prod. Res. 22 (2008) 709–714.

[38] J.D. Johnson, L.A. Wittenauer, A fluorescent calmodulin that reports the binding of hydrophobic inhibitory ligands, Biochem. J. 211 (1983) 473–479.

[39] W.L. DeLano, Use of PYMOL as a communications tool for molecular science, Abstracts Papers Am. Chem. Soc. 228 (2004) U313–U314.

[40] M.A. Andrade, P. Chacon, J.J. Merelo, F. Moran, Evaluation of secondary structure of proteins from UV circular dichroism spectra using an unsupervised learning neural network, Protein Eng. 6 (1993) 383–390.